Appl. Phys. B (2016) 122:20
DOI 10.1007/s00340-015-6284-9

Applied Physics B
Lasers and Optics

Single telecom photon heralding by wavelength multiplexing in an optical fiber

Andreas Lenhard[1] · **José Brito**[2] · **Stephan Kucera**[2] · **Matthias Bock**[1] · **Jürgen Eschner**[2] · **Christoph Becher**[1]

Received: 28 May 2015 / Accepted: 2 November 2015 / Published online: 22 January 2016

Abstract We demonstrate the multiplexing of a weak coherent and a quantum state of light in a single telecommunication fiber. For this purpose, we make use of spontaneous parametric down conversion and quantum frequency conversion to generate photon pairs at 854 nm and the telecom O-band. The herald photon at 854 nm triggers a telecom C-band laser pulse. The telecom single photon (O-band) and the laser pulse (C-band) are combined and coupled to a standard telecom fiber. Low-background time correlation between the weak coherent and quantum signal behind the fiber shows successful multiplexing.

1 Introduction

Today's Internet traffic that is distributed over optical fiber channels mainly concentrates on the telecom C- (1530–1565 nm) and L-band (1565–1625 nm) because in-line active amplifiers based on erbium-doped fibers offer a feasible way to build repeaters for the signals. Hence, there exist a number of telecom frequency bands which are not used, being available for quantum communication.

In state-of-the-art realizations, quantum key distribution (QKD) is possible over 336 km [1] and entanglement distribution was demonstrated with lengths up to 300 km [2]. QKD with such high-loss channels became possible only with the development of low-noise detectors [3]. Based on this progress, QKD over existing fiber networks in urban areas has been demonstrated [4–6] as well as entanglement distribution [7] and teleportation [8].

QKD protocols, e.g., BB84 [9], usually involve an exchange of data via a quantum and a classical channel simultaneously to establish the final secret key. Realizing both channels in a single fiber reduces the demand for fiber infrastructure at the cost of slightly increasing the device complexity at sending and receiving stations. In first experimental demonstrations, weak coherent pulses at the single-photon power level in the telecom O-band (1260–1360 nm) were multiplexed with a common data channel in the C-band and sent via several kilometers of installed fiber [10] with an acceptable error rate of the quantum channel. The dominant noise source in that scheme is anti-Stokes Raman scattering of the strong classical pulses into the quantum channel [11]. Furthermore, it is also possible to transmit the O-band photons through a fiber link equipped with active erbium amplifiers. The spontaneous emission of the amplifiers at O-band wavelengths is quite low, and the amount of additional noise photons in the quantum channel can be neglected after narrow spectral filtering [12]. However, each amplifier attenuates the O-band photons (e.g., 11 dB loss in [12]). Nevertheless, in such a configuration, the distribution of entangled states was demonstrated [12]. In recent work [13], a scheme was presented where the amplifiers were bypassed and noise in the O-band was investigated in detail.

The telecom C-band is divided into a grid of equally spaced channels for dense wavelength multiplexing (12.5–100 GHz spacing in ITU-grid [14]). Each of these channels can be used independently for classical communication, and filters are available to separate and demultiplex

---

This paper is part of the topical collection "Quantum Repeaters: From Components to Strategies" guest edited by Manfred Bayer, Christoph Becher and Peter van Loock.

✉ Christoph Becher
christoph.becher@physik.uni-saarland.de

[1] Quantenoptik, Fachrichtung 7.2, Universität des Saarlandes, Campus E2.6, 66123 Saarbrücken, Germany

[2] Quantenphotonik, Fachrichtung 7.2, Universität des Saarlandes, Campus E2.6, 66123 Saarbrücken, Germany

individual channels. However, the suppression of such common filters is not high enough (20–40 dB) to protect a quantum channel from neighboring classical states of light. If such a fiber link includes an amplifier, a quantum channel in the C-band will also be classically amplified which destroys its quantum state (no cloning theorem). From these considerations, transmitting the quantum channel in the O-band (taking losses into account) and classical data in the C-band seems the best solution.

To establish a quantum network, quantum nodes like single trapped atoms or ions, emitting in the visible or near infrared spectral region, have to be interconnected via photons. To this end, bridging the gap between low-loss telecom wavelengths for long-range communication and the atomic wavelengths quantum frequency conversion (QFC) is necessary [15–17]. In the present experiment, we produce frequency-degenerate photon pairs, generated by spontaneous parametric down conversion (SPDC), resonant with an atomic transition of ^{40}Ca^{+} at 854 nm. One of these photons is frequency converted to the telecom O-band. Its partner photon triggers a telecom C-band laser pulse which is overlapped with the converted photon and transmitted through a long single-mode fiber. This means we here multiplex a quantum state of light at a wavelength in the telecom O-band with a coherent light field in the telecom C-band. We measure time correlations between the laser pulse and the converted photon at the fiber output, which arise from the original non-classical time correlation of the SPDC pair, maintained along frequency conversion, multiplexing and fiber transmission. This technique is also a proof of principle for all-optical distribution of a signal for heralding single photons.

2 Fiber characterization

To examine the different properties of fibers in the O- and C-band in a preliminary experiment, we use correlated photon pairs in each of these bands. For this purpose, we pump a lithium niobate waveguide [18] at a wavelength of 708 nm to generate SPDC photons at 1535 and 1313 nm with sinc^2-shaped spectrum and a bandwidth of approximately 870 GHz (FWHM), respectively (details about SPDC in this particular device can be found in [18]). Both photons are sent through long single-mode fibers (SMF-28e) before separating them with a wavelength division multiplexer (WDM). Each output of the WDM is connected to a single-photon detector. In the post-processing of the data, we correlate the arrival times of the photons to measure the coincidences between O-band and C-band photons. The fiber has a different refractive index in the O- and C-band, and thus, the delay between the photons will depend on the length of the fiber. Hence, the position of the coincidence peak will move. The result is shown in Fig. 1. As we used the same measurement time for all fiber lengths, the total number of coincidences reduces due to losses. Additionally, due to the broadening, the coincidences are spread over a larger number of time bins in the graph. Both effects result in an increased measurement uncertainty and reduced signal-to-background ratio, assuming a square root error model for the number of coincidences. This becomes visible in the broadening of the curves in the figure. We attribute the side peaks visible for fiber lengths above 20 km to reflections in the optical path.

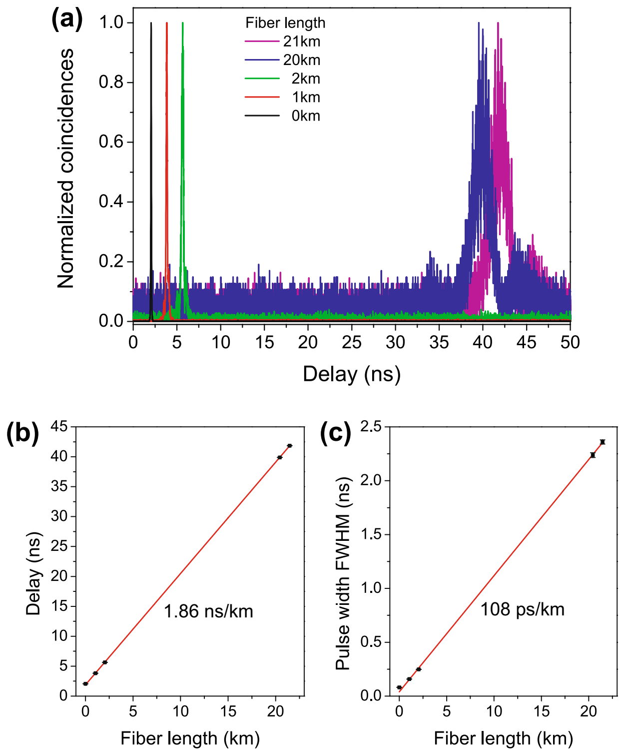

Fig. 1 Dispersion effects in the telecom fiber. **a** Shows correlation measurements between O-band and C-band photon pairs sent through different fibers. **b** Shows the shift of the coincidence peak and **c** the broadening of this peak for the different fibers. The *red solid lines* in **b** and **c** are linear fits to the experimental data

Furthermore, even the individual spectral components of each photon will experience different phase velocities leading to pulse broadening. The dispersion minimum of SMF-28 fibers is in the telecom O-band ($1310 < \lambda_0 < 1324$ nm, [19]). Hence, we expect negligible pulse broadening there, but the temporal shape of the C-band photon will significantly broaden due to dispersion. The results of the correlation measurement show that the delay between the O-band and C-band photons increases by 1.861 ± 0.004 ns/km. This value was measured at the peak positions and thus holds for every pulse pair with 1535 and 1313 nm central wavelength. With the help of the effective group refractive indices of the optical fiber given in the data sheet [19] ($n_{1310} = 1.4676$, $n_{1550} = 1.4682$), we estimate a dispersion of 2 ns/km, in agreement with our experimental findings. For the pulse broadening of the C-band photons, we find a value of 108 ± 0.8 ps/km which depends on the particular spectral shape. Again we can estimate a value from the parameters given in the data sheet [19]. The dispersion is given as ≤ 18.0 ps/(nm·km). A FWHM of 870 GHz corresponds to a spectral bandwidth of 7 nm, resulting in a dispersion of ≤ 126 ps/km. This is compatible with our measurement results.

In practical realizations, such effects can hamper the applicability. In Internet communication, the link between two nodes can be reconfigured on demand to reduce data traffic in certain channels and optimize speed and workload. Hence, the optical distance between two nodes might change. For the idea of multiplexing quantum and classical channels, this means the delay between these data packets might also change. There exist techniques to synchronize measurements which were referenced to independent clocks via the time correlation of photon pairs [20]. A similar algorithm could be implemented here to track the correlation signal.

3 Quantum and classical signal in a single fiber

To demonstrate the multiplexing of two optical signals in a single fiber (SMF-28e), we implemented the experiment described in the following and shown in Fig. 2.

We use spontaneous parametric down conversion (SPDC) to generate photon pairs at 854 nm. This source has been described earlier in more detail [21, 22] where it has been used to herald the absorption of a single photon by a single trapped ion. It consists of a diode laser system at 854 nm which is actively stabilized to an atomic transition in calcium ($^{40}\text{Ca}^+$, $3^2\text{D}_{5/2} \leftrightarrow 4^2\text{P}_{3/2}$). The second harmonic (SHG) of this laser field serves as pump field for the SPDC process. This allows to generate frequency-degenerate photons resonant with the transition in Ca^+. The down conversion is realized via type II phase-matching conditions in a 2-cm-long periodically poled KTP (PPKTP) crystal. The photons are thus polarization entangled. However, for the experiments reported here, this kind of entanglement is not used and we employ a polarizing beam splitter (PBS) to effectively separate the signal and idler photons. One photon serves as a herald, which is detected by a silicon avalanche photon detector (Si-APD, Perkin Elmer SPCM-AQR-14, 30 % detection efficiency at 854 nm), while its partner photon is sent to the frequency converter setup. For frequency conversion, we make use of difference frequency generation in a periodically poled lithium niobate ridge waveguide (similar to the device described in [16]). The conversion from $\lambda_s = 854$ nm to the telecommunications O-band around $\lambda_i = 1310$ nm is stimulated by a strong coherent pump field at a wavelength of $\lambda_p = 2453$ nm ($1/\lambda_s - 1/\lambda_p = 1/\lambda_i$). This pump field is generated by a continuous wave optical parametric oscillator (OPO). From calibration measurements, we determine the overall conversion efficiency to approximately 8 % (including coupling of signal photons to the waveguide and telecom photons to the output fiber). Finally, we use superconducting single-photon detectors (SSPD, Single Quantum EOS X10) for counting the telecom photons (detection efficiency of 25 % at 1310 nm). Although the efficiency of frequency conversion is only 8 % here, the overall transmission efficiency (including conversion and fiber transmission losses) benefits from the small fiber losses in the O-band (measured as 0.25 dB/km at 1310 nm, compared to approx. 2 dB/km at 854 nm) and equals the transmission efficiency of the unconverted photons at a fiber length of 6.5 km. After 20 km of fiber, the advantage of the conversion scheme amounts to 24 dB. These numbers illustrate that low-loss transmission of quantum states through fibers benefits from QFC.

To multiplex classical and quantum states of light in a single fiber, we connect the heralding detector (Si-APD) to a diode laser (Thorlabs LPSC-1550-DC) emitting at 1550 nm in the telecom C-band. In detail, the diode was biased with a DC current of 11 mA and the TTL pulses were added via a bias-T and a 50 Ohm load resistor. This is enough to drive the diode above threshold (36 mA). The bias current reduces fluctuations of the pulse shape without finally introducing excess noise by continuous photons.

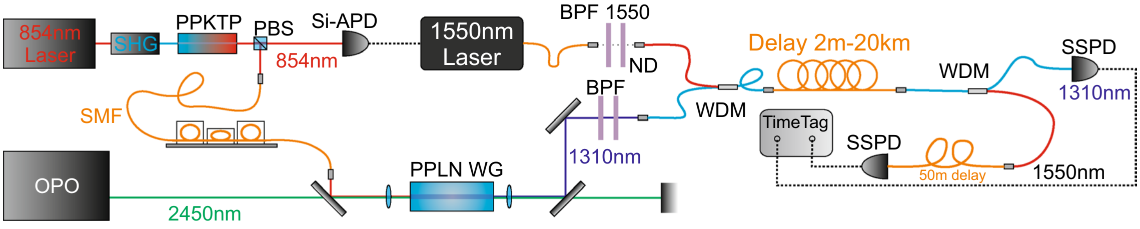

Fig. 2 Experimental setup for correlation measurements between converted photons and an optical clock signal. For abbreviations see text

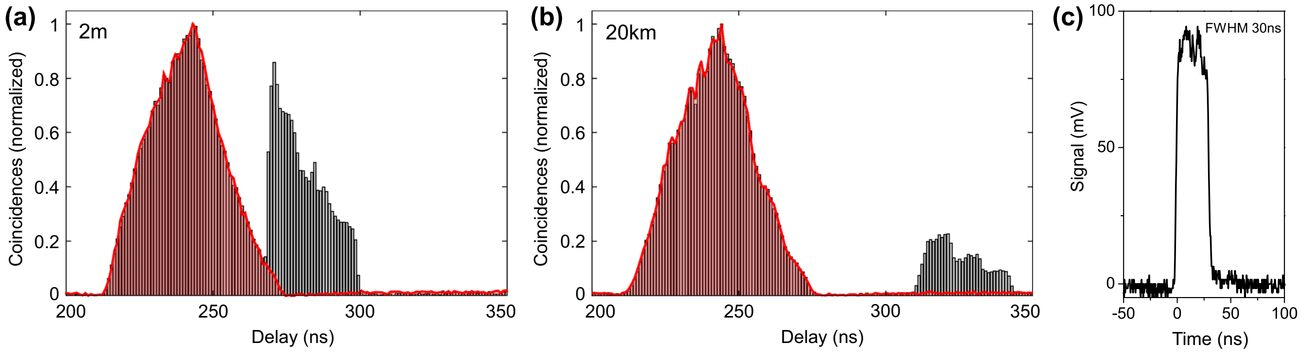

Fig. 3 Converted single photons at telecom O-band and laser herald pulses in the telecom C-band multiplexed in a single fiber. **a** Shows the results for 2 m of delay, as reference, and **b** shows the long-range measurement over 20 km. The *red solid lines* show measurements of the background, and the *gray bars* show the measurement results including O-band single photons. The *red shaded areas* are a guide for the eye and indicate the cross-talk coincidences of the laser pulses. Detections in the O-band channel were used as start and in the C-band channel as stop triggers for the correlation measurements. **c** Shows a measurement of the laser pulse intensity with a standard photodiode and an oscilloscope (2 m fiber delay)

The shape of the generated optical pulse (Fig. 3c) follows the electrical current. The laser pulse is transmitted through 1550-nm bandpass filters (BPF, 20 nm FWHM) to suppress noise at other telecom wavelengths, generated by the laser. Then, the pulses are sent to the laboratory where the converter is hosted. There, the laser pulses are combined with the converted photons via a WDM as shown in Fig. 2. After combination, both optical fields travel in the same delay fiber which can be set to various lengths between 2 m and 20 km. After this fiber link, both fields are again separated by a single WDM. These WDMs (Thorlabs WD202B-FC) have a minimal isolation of 16 dB between the two bands. We first performed the correlation measurement with non-attenuated laser pulses and additional filters before the single-photon detector at the O-band. In this case, we were able to detect the C-band laser pulses with a standard photodiode (Thorlabs DET10C), thus proving that single-photon sensitivity is not necessary in the clock channel. Unfortunately, the background in the single-photon O-band channel drastically increased due to channel cross talk. With this configuration, we were not able to clearly prove the preservation of the temporal correlation between the single photons and the laser pulses. The experimental setup could be optimized by including narrowband filters (e.g., fiber bragg gratings) and WDMs with higher isolation. A similar result was observed in a recent paper where Raman scattering of the strong pulses was identified as main noise source [13].

One way to reduce this noise is to reduce the power of the laser pulses and use detectors with higher sensitivity. Superconducting single-photon detectors are a current state-of-the art technology to register single photons. Their advantage is a low timing jitter in the order of 50 ps and high detection efficiency at telecom wavelengths. As we already use such a device for the O-band channel, the system complexity only marginally increases by adding a second device for the C-band channel. To observe the temporal correlations between O-band and C-band signals, we thus reduce the power of the C-band pulses by adding neutral density filters and connect both output channels to the SSPDs, as shown in Fig. 2. The C-band channel has an additional delay of 50 m of fiber to reduce cross-talk effects in detection. In a preparatory measurement, the rate of herald events was measured directly at the Si-APD. Then, the laser pulses were attenuated by six orders of magnitude which, for the heralding channel, resulted in a comparable count rate on the SSPD as on the Si-APD before. We collect the detection events on both SSPD in a list of time stamps using a fast counting electronics (Roithner Laser TTM8000) and correlate both later. For comparison, a background measurement was performed by blocking the input of 854 nm photons in the converter and repeating the measurements with the same settings (red curves in Fig. 3). When the laser pulses arrive at the WDM, the major part is directed to the C-band output port. However, a small fraction of the pulse (given by the WDM isolation) will also be directed to the O-band port. As the coherent pulse consists of many photons, this leakage results in a coincidence detection on both detectors. The shape of this coincidence peak is given by the autocorrelation of the laser pulse, and the position of the peak is given by the difference in optical delay between the WDM and the individual detectors. The background measurement makes this effect visible as the true single-photon signal is blocked. Furthermore, we expect a very low constant noise floor by accidental coincidences between telecom O-band noise photons generated in the converter and C-band spontaneous emission of the laser, as well as detector dark counts in both channels. The laser pulses have a rectangular shape of 30 ns width (see Fig. 3c). Hence, we expect a triangular autocorrelation with a width of 60 ns at the base. This corresponds well with the experimental width of 62 ns. The results for simultaneous transmission of classical and quantum signals are shown as gray bars in Fig. 3(a, b) for the shortest and longest available fiber lengths, respectively.

In both examples, we can identify two coincidence peaks. We inserted an additional 50 m delay fiber between the two SSPD channels (measured to introduce 244 ns delay). Hence, we can identify the peak around 240 ns to stem from the fraction of the C-band laser pulse leaking into the O-band detection channel. This is proved by the background coincidence rate (red lines in Fig. 3) which shows that this peak is completely independent of the frequency converted photons. In contrast, the neighboring peak (gray shaded area) stems from the correlation between the laser pulses and the converted single photons. The center of mass of this peak shifts by 43 ns which is comparable to the shift expected from the earlier results (37.2 ns for 20 km, see Fig. 1). For the correlation signal of interest, we expect a convolution between the short photon pulse (coherence time 5 ps) and the laser pulse (30 ns). The measured width at the base of the 20 km delayed pulse is 34 ns, corresponding well with the estimated value (30 ns $+$ 20 km$\cdot$108 ps/km $=$ 32 ns). We can attribute the modulation of the pulse height to saturation and dead-time effects in the detectors. The coherent laser pulse consists of more than one photon on average which means that possibly more than one detection event can be triggered by a single pulse on the SSPD. In particular, the dead time of the SSPD is around 10 ns which is shorter than the pulse width, giving rise to the threefold peak structure of the 30 ns long coincidence peak.

An effective separation of the signal of interest and the background is possible by gated detection, where the position and width of the gate window are adapted to position and shape of the signal coincidence peak.

4 Conclusion

To summarize the results, we have shown a basic experiment demonstrating a way to multiplex classical and quantum channels in a single fiber. We demonstrated the correlation of the SPDC photons by transmitting the timing information by an optical clock pulse in the telecom C-band. Moreover, we used quantum frequency conversion to the telecom O-band to tackle the high transmission losses of quantum-memory compatible photons. Both QFC and mapping of the detection event to a laser pulse preserve the time correlation of the original 854 nm partner photons. This is an important proof-of-principle demonstration for distribution of quantum information using existing fiber network infrastructure.

Regarding a practical application, we should use gated detection and choose the gate width and position to cut out the coincidence peak with the true signal only, thereby discarding the detection channel cross-talk effects we observed. For fibers with several kilometers of length, the delay is large enough to make this feasible. The laser pulses used in this proof-of-principle demonstration were generated by direct electrical connection of the APD to the laser. A further improvement is to use much shorter laser pulses that decrease timing jitter as well as reduce dead-time effects in detection. Together with the gating, this would decrease noise background. As pointed out in a recent publication temporal gating combined with spectral filtering makes multiplexing of a quantum channel and a standard communication channel in a single fiber feasible [13]. Those improvements can also be applied to our scheme.

Acknowledgments The work was funded by the German Federal Ministry of Science and Education (BMBF) within the projects “Q.com-Q” (Contract No. 16KIS0127). J. Brito acknowledges support by CONICYT.

References

1. H. Shibata, T. Honjo, K. Shimizu, Quantum key distribution over a 72 dB channel loss using ultralow dark count superconducting single-photon detectors. Opt. Lett. **39**, 5078–5081 (2014)
2. T. Inagaki, N. Matsuda, O. Tadanaga, M. Asobe, H. Takesue, Entanglement distribution over 300 km of fiber. Opt. Express **21**, 23241–23249 (2013)
3. H. Takesue, S. Nam, Q. Zhang, R.H. Hadfield, T. Honjo, K. Tamaki, Y. Yamamoto, Quantum key distribution over a 40-dB channel loss using superconducting single-photon detectors. Nat. Photonics **1**, 343–348 (2007)
4. M. Peev, C. Pacher, R. Alleaume, C. Barreiro, J. Bouda, W. Boxleitner, T. Debuisschert, E. Diamanti, M. Dianati, J.F. Dynes, S. Fasel, S. Fossier, M. Fürst, J.-D. Gautier, O. Gay, N. Gisin, P. Grangier, A. Happe, Y. Hasani, M. Hentschel, H. Hübel, G. Humer, T. Länger, M. Legre, R. Lieger, J. Lodewyck, T. Lorünser, N. Lütkenhaus, A. Marhold, T. Matyus, O. Maurhart, L. Monat, S. Nauerth, J.-B. Page, A. Poppe, E. Querasser, G. Ribordy, S. Robyr, L. Salvail, A.W. Sharpe, A.J. Shields, D. Stucki, M. Suda, C. Tamas, T. Themel, R.T. Thew, Y. Thoma, A. Treiber, P. Trinkler, R. Tualle-Brouri, F. Vannel, N. Walenta, H. Weier, H. Weinfurter, I. Wimberger, Z.L. Yuan, H. Zbinden, A. Zeilinger, The SECOQC quantum key distribution network in Vienna. New J. Phys. **11**, 075001 (2009)
5. M. Sasaki, M. Fujiwara, H. Ishizuka, W. Klaus, K. Wakui, M. Takeoka, S. Miki, T. Yamashita, Z. Wang, A. Tanaka, K. Yoshino, Y. Nambu, S. Takahashi, A. Tajima, A. Tomita, T. Domeki, T. Hasegawa, Y. Sakai, H. Kobayashi, T. Asai, K. Shimizu, T. Tokura, T. Tsurumaru, M. Matsui, T. Honjo, K. Tamaki, H. Takesue, Y. Tokura, J.F. Dynes, A.R. Dixon, A.W. Sharpe, Z.L. Yuan, A.J. Shields, S. Uchikoga, M. Legre, S. Robyr, P. Trinkler, L. Monat, J.-B. Page, G. Ribordy, A. Poppe, A. Allacher, O. Maurhart, T. Länger, M. Peev, A. Zeilinger, Field test of quantum

key distribution in the Tokyo QKD Network. Opt. Express **19**, 10387–10409 (2011)
6. A. Rubenok, J.A. Slater, P. Chan, I. Lucio-Martinez, W. Tittel, Real-world two-photon interference and proof-of-principle quantum key distribution Immune to detector attacks. Phys. Rev. Lett. **111**, 130501 (2013)
7. W. Tittel, J. Brendel, H. Zbinden, N. Gisin, Violation of bell inequalities by photons more than 10 km apart. Phys. Rev. Lett. **81**, 3563–3566 (1998)
8. I. Marcikic, H. de Riedmatten, W. Tittel, H. Zbinden, N. Gisin, Long-distance teleportation of qubits at telecommunication wavelengths. Nature **421**, 509–513 (2003)
9. C.H. Bennett, G. Brassard, in International Conference on Computers, Systems and Signal Processing (Bangalore, 1984), pp. 175–179
10. P.D. Townsend, Simultaneous quantum cryptographic key distribution and conventional data transmission over installed fibre using wavelength-division multiplexing. Electr. Lett. **33**, 188–190 (1997)
11. T.E. Chapuran, P. Toliver, N.A. Peters, J. Jackel, M.S. Goodman, R.J. Runser, S.R. McNown, N. Dallmann, R.J. Hughes, K.P. McCabe, J.E. Nordholt, C.G. Peterson, K.T. Tyagi, L. Mercer, H. Dardy, Optical networking for quantum key distribution and quantum communications. New J. Phys. **11**, 105001 (2009)
12. M.A. Hall, J.B. Altepeter, P. Kumar, Drop-in compatible entanglement for optical-fiber networks. Opt. Express **17**, 14558–14566 (2009)
13. S. Aleksic, F. Hipp, D. Winkler, A. Poppe, B. Schrenk, G. Franzl, Perspectives and limitations of QKD integration in metropolitan area networks. Opt. Express **23**, 10359–10373 (2015)
14. International Telecommunication Union, Spectral grids for WDM applications: DWDM frequency grid, ITU-T G.694.1, version 02/2012
15. Z.Y. Ou, Efficient conversion between photons and between photon and atom by stimulated emission. Phys. Rev. A **78**, 023819 (2008)
16. S. Zaske, A. Lenhard, C.A. Keßler, J. Kettler, C. Hepp, C. Arend, R. Albrecht, W.-M. Schulz, M. Jetter, P. Michler, C. Becher, Visible-to-telecom quantum frequency conversion of light from a single quantum emitter. Phys. Rev. Lett. **109**, 147404 (2012)
17. S. Blum, G.A. Olivares-Renteria, C. Ottaviani, C. Becher, G. Morigi, Single-photon frequency conversion in nonlinear crystals. Phys. Rev. A **88**, 053807 (2013)
18. M. Bock, A. Lenhard, C. Becher, A highly efficient heralded single photon source for telecom wavelengths based on a PPLN ridge waveguide (2016) (Manuscript in preparation)
19. Corning SMF-28e+ Optical Fiber with NexCor Technology—Product Information, Document PI1463, December 2007, Corning Inc
20. C. Ho, A. Lamas-Linares, C. Kurtsiefer, Clock synchronization by remote detection of correlated photon pairs. New J. Phys. **11**, 045011 (2009)
21. N. Piro, A. Haase, M.W. Mitchell, J. Eschner, An entangled photon source for resonant single-photon-single-atom interaction. J. Phys. B At. Mol. Opt. Phys. **42**, 114002 (2009)
22. N. Piro, F. Rohde, C. Schuck, M. Almendros, J. Huwer, J. Ghosh, A. Haase, M. Hennrich, F. Dubin, J. Eschner, Heralded single-photon absorption by a single atom. Nat. Phys. **7**, 17–20 (2010)